Orientation and relaxation in uniaxially stretched poly(methyl methacrylate)–poly(ethylene oxide) blends

Y. Zhao, B. Jasse* and L. Monnerie

Laboratoire de Physico-chimie Structurale et Macromoléculaire, associé au CNRS, Ecole Supérieure de Physique et de Chimie Industrielles de la Ville de Paris, 10 rue Vauquelin, 75231 Paris Cedex 05, France

(Received 1 December 1988; revised 23 January 1989; accepted 25 January 1989)

Uniaxial orientation of poly(methyl methacrylate) (PMMA) and poly(ethylene oxide) (PEO) chains in their compatible blends has been measured using infra-red dichroism and birefringence. The influence of strain rate, temperature of stretching and PEO molecular weight on orientation of both polymer chains in blends containing up to 20% PEO has been studied. Mechanical relaxation master curves at a reference temperature $T = T_g + 50°C$ have also been determined. The results are interpreted in terms of a hindrance of relaxation of PMMA chains induced by a modification of friction coefficients due to the molecular interactions that are at the origin of compatibility.

(Keywords: poly(methyl methacrylate); poly(ethylene oxide); polymer blends; orientation; relaxation; Fourier-transform infra-red; birefringence)

INTRODUCTION

In previous work[1–6] on various compatible blends based on polystyrene (PS) we pointed out that, in PS–PPO (poly(2,6-dimethyl-1,4-phenylene oxide)) blends and in PS–PVME (poly(vinyl methyl ether)) blends, chains orient in a different way when subjected to a uniaxial strain in spite of the compatible nature of the blend. In PS–PPO blends a similar behaviour is observed for both polymers. Orientation is concentration-dependent when the corresponding component is present in a large amount[6] and one can observe a linear increase of the orientation up to a limit concentration C_1. Actually $C_1 \simeq 20\%$ of PPO for PS orientation and $C_1 \simeq 25\%$ of PS for PPO orientation. Between these two values, orientation of both components is insensitive to the composition of the blend.

In PS–PVME blends[4], up to a concentration of 25% of PVME, PS orientation increases with PVME concentration while PVME remains almost unoriented. In PS–poly(*o*-chlorostyrene) blends[5] both polymers orient in a similar way. All these results were satisfactorily interpreted in terms of hindrance of relaxation of PS chains induced by a modification of friction coefficients due to the molecular interactions that are at the origin of compatibility.

It was interesting to examine the behaviour of a compatible blend based on another polymer and the present work deals with the study of orientation and relaxation of poly(methyl methacrylate)–poly(ethylene oxide) (PMMA–PEO) blends using infra-red dichroism, birefringence and dynamic shear measurements.

COMPATIBILITY OF PMMA–PEO BLENDS

The compatibility of PMMA–PEO blends, which was theoretically predicted[7], was effectively observed experimentally in the melt state by Martuscelli *et al.*[8–11] in PMMA–PEO blends containing more than 60% of PEO, using thermal analysis, optical and electronic microscopy and X-ray diffraction. On the other hand, PEO chain mobility in melt blends characterized by the spin–lattice relaxation time T_1 was measured by carbon-13 n.m.r.[12] and shown to be strongly reduced by the presence of PMMA chains. In a polymer blend in which one of the components may crystallize, which is presently the case of PEO, melting temperature depression results from compatibility and allows one to evaluate the Flory–Huggins interaction parameter χ_{12} (ref. 13). The values of this parameter obtained by different authors and given in *Table 1* show that PMMA–PEO blends are thermodynamically stable in the melt state. However, it is important to note that Alfonso and Russell[16] using the same method obtained a value of $\chi_{12} \simeq 0$.

In the solid state, the crystallization behaviour of PEO is influenced by PMMA. Up to a content of about 40 wt% of PMMA the blend films are completely filled with PEO spherulites, the PMMA molecules being incorporated in interlamellar regions of PEO spherulites[10,15,17].

When PMMA concentration increases, phase separation may occur, resulting in crystallites coexisting with two amorphous phases[18]. At least, no crystallization is observed in blends containing less than 20% of PEO; the glass transition temperature of the samples being

Table 1 Values of the Flory–Huggins parameter χ_{12} in PMMA–PEO blends

PEO $\bar{M}_w$	PMMA $\bar{M}_w$	T(°C)	χ_{12}	Ref
4.00×10^6	9.36×10^4	60	−0.131	14
3.56×10^5	9.36×10^4	60	−0.139	14
4.00×10^3	6.00×10^5	60	−0.157	15
1.00×10^5	1.10×10^5	74	−0.35	10
		76	−1.93	8

* To whom correspondence should be addressed

0032-3861/89/091643-08$03.00

Table 2 Characteristics of PEO samples

Sample	$\bar{M}_w$	Origin
PEO 06	600	Merck-Schuchardt
PEO 1	1000	Merck-Schuchardt
PEO 2	2000	Merck-Schuchardt
PEO 4	4000	Merck-Schuchardt
PEO 20	20000	Merck-Schuchardt
PEO 50	50000	Merck-Schuchardt
PEO 200	200000	Polysciences Inc.
PEO 600	600000	Polysciences Inc.

Table 3 Glass transition temperatures (°C) for each blend

	PEO (%)			
Blend	5	10	15	20
PMMA–PEO 06	96	84		
PMMA–PEO 1	98	84		
PMMA–PEO 2	98	91		
PMMA–PEO 4	98	91		70
PMMA–PEO 20	98	91	78	70
PMMA–PEO 50	98	91		70
PMMA–PEO 200	98	91		
PMMA–PEO 600	98	91		

above the crystallization temperature, the blends are amorphous, transparent and present only one glass transition temperature[15,19]. As we are presently concerned with compatible blends in the amorphous state, our study was limited to samples containing up to 20% of PEO.

EXPERIMENTAL

The PMMA used was a pure polymer obtained by radical chain polymerization, while PEO samples were commercial products. Their characteristics are given in *Table 2*.

Sample preparation

Thin films suitable for infra-red spectroscopy were obtained by casting a 6% chloroform solution on a glass plate. Subsequent annealing was done under vacuum for 30 h at 100°C in order to remove any trace of solvent and internal stress. Samples for mechanical measurements were compression-moulded. The glass transition temperatures of the samples were obtained using a DuPont 1090 differential scanning calorimeter at a heating rate of 20°C min^{-1}; sample weight was ~7 mg. T_g values for each blend are given in *Table 3*.

Oriented samples from thin films were obtained on an apparatus developed in our laboratory[20], i.e. a stretching machine operating at constant strain rate and a special oven to obtain a very good stability of the temperature over all the sample (homogeneity is ~0.05°C).

Infra-red dichroism

The polarized spectra were recorded using a Nicolet 7199 Fourier-transform infra-red spectrometer. A gold-wire-grid Specac polarizer set at maximum transmission position was used and the samples rather than the polarizer were rotated by 90° in order to obtain the two polarization measurements. A total of 32 co-added interferograms were scanned at 2 cm^{-1} resolution. Infra-red dichroism was calculated as $R = A_{\parallel}/A_{\perp}$ for the peak optical densities $A_{\parallel}$ and $A_{\perp}$.

Birefringence

Birefringence was measured at a wavelength of 0.59 μm using a birefringence modulator which allows one to measure a low level of birefringence with fairly good precision[21,22]. The thickness of each sample was obtained with a Modular 2520/D comparator and averaged along the specimen.

Dynamic shear

A Rheometrics Weissenberg-type RMS 605 rheometer fitted with a cone–plate system (25 mm diameter; angle 0.155 rad) was used. The frequency range was 10^{-2} to 10^{+2} rad s^{-1}.

RESULTS

Orientation behaviour

Dichroic ratio measurements allow one to calculate the second-order moment of the orientation function according to the relation:

$$\langle P_2(\cos\theta)\rangle = \tfrac{1}{2}(3\langle\cos^2\theta\rangle - 1) = \frac{R-1}{R+2}\frac{R_0+2}{R_0-1}$$

with $R_0 = 2\cot^2\alpha$ where α is the angle between the dipole moment vector of the considered vibration and the chain axis and θ is the angle between the chain axis and the draw direction[23]. Although infra-red spectroscopy is an attractive method of deducing the chain orientations of the different polymers in a blend, absorption band overlapping may restrict the possibility of analysis. As shown from the PMMA and PEO spectra given in *Figure 1*, absorption bands of both polymers badly overlap and only PMMA orientation can be measured using the 749 cm^{-1} absorption band, which is assigned to a skeletal vibrational motion affected by the CH_2 rocking vibration[24]. The angle α of the dipole moment vector of this vibration was measured at 17° (ref. 25). The knowledge of PMMA orientation allows one to estimate PEO orientation from birefringence measurements.

As a matter of fact birefringence Δ in an oriented compatible blend is related to individual orientation functions[26] by the relation:

$$\Delta = f_1\Delta_1^0\langle P_2(\cos\theta)\rangle_1 + f_2\Delta_2^0\langle P_2(\cos\theta)\rangle_2$$

where f_i, Δ_i^0 and $\langle P_2(\cos\theta)\rangle_i$ are the volume fraction, intrinsic birefringence and orientation function of component i, respectively.

PMMA orientation

All the samples were stretched at constant strain rate above the glass transition temperature. First consider the results obtained at a stretching temperature $T = T_g + 21$°C and a strain rate $\dot{\varepsilon} = 0.026\ s^{-1}$ for different PMMA–PEO blends.

Figure 2 shows the change of the $\langle P_2(\cos\theta)\rangle$ orientation function relative to PMMA as a function of draw ratio and PEO percentage in the blend. A rectilinear relation holds for any composition of the blend between $\langle P_2(\cos\theta)\rangle$ *versus* draw ratio.

It is interesting to describe the orientation behaviour

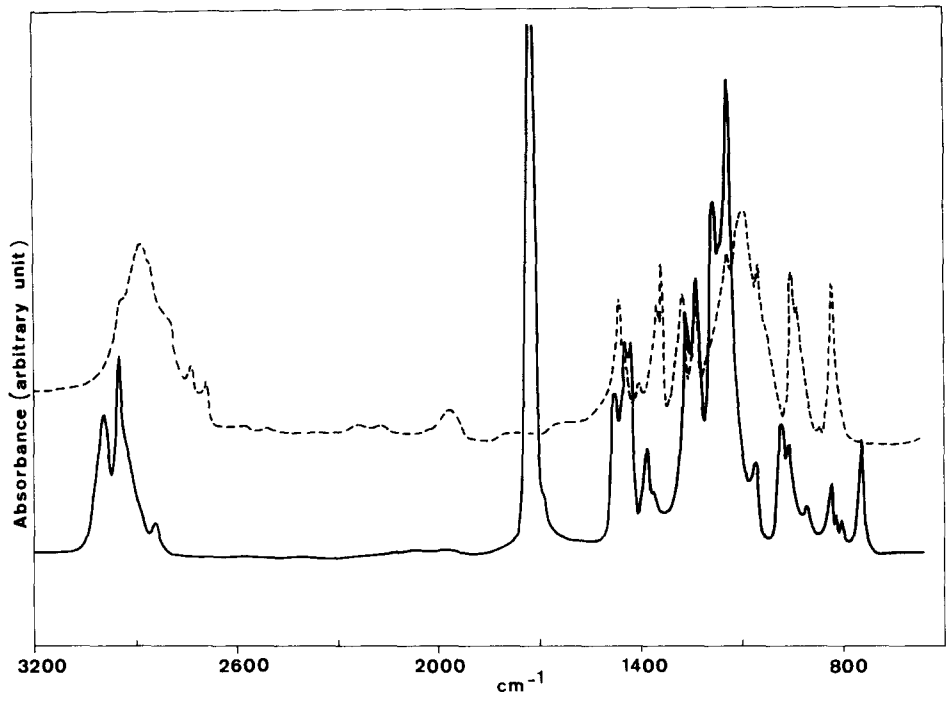

Figure 1 Infra-red spectra of PMMA (——) and PEO (– – – –)

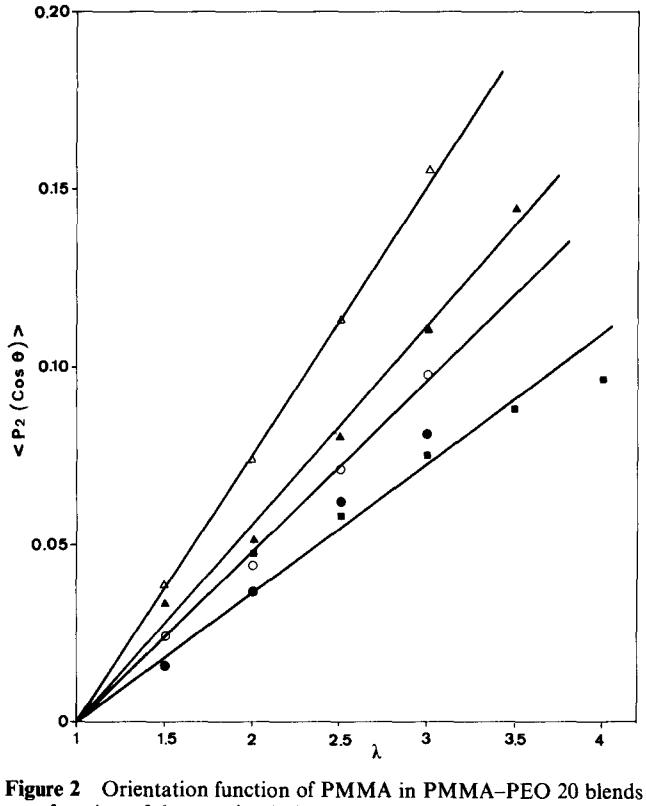

Figure 2 Orientation function of PMMA in PMMA–PEO 20 blends as a function of draw ratio: (■) pure PMMA; (△) blend 5% (PEO: (▲) blend 10% PEO; (○) blend 15% PEO; (●) blend 20% PEO. Temperature of stretching $T = T_g + 21°C$. Strain rate $\dot{\varepsilon} = 0.026\,s^{-1}$

by plotting the slope $d\langle P_2(\cos\theta)\rangle/d\lambda$ as a function of PEO percentage. *Figure 3* shows that a strong increase of PMMA orientation with respect to the pure polymer occurs in the blend containing 5% of PEO. Then orientation decreases progressively with an increasing amount of PEO. Orientation of PMMA in the 20% PEO blend is identical to pure PMMA stretched under the same conditions.

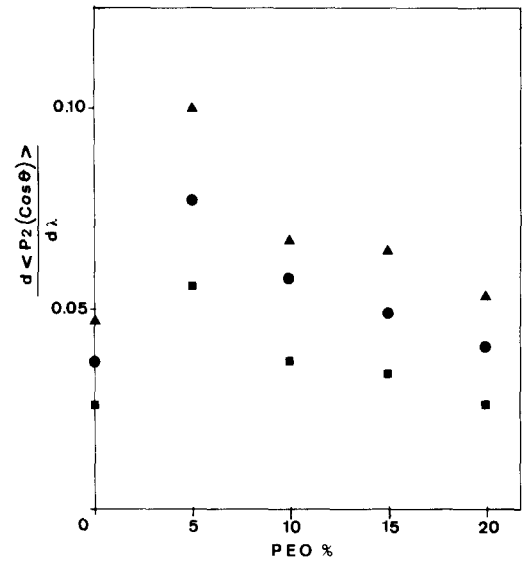

Figure 3 Slope of $\langle P_2(\cos\theta)\rangle_{PMMA} = f(\lambda)$ as a function of PEO 20 percentage. Strain rate $\dot{\varepsilon}$: (■) $0.008\,s^{-1}$; (●) $0.026\,s^{-1}$; (▲) $0.115\,s^{-1}$. Temperature of stretching $T = T_g + 21°C$

The influence of strain rate on PMMA orientation in the blends is also shown in *Figure 3*. Orientation increases with strain rate. As expected from the time–temperature equivalence, similar behaviour is observed when the stretching temperature is closer to T_g as shown in *Figure 4*.

In addition to the stretching parameters (λ, T, $\dot{\varepsilon}$) it is interesting to examine the influence on PMMA orientation of the molecular weight of PEO. *Figure 5* shows the change of PMMA orientation function as a function of draw ratio for different PEO molecular weights in blends containing 5% of PEO. In all the samples, PMMA orientation is higher than pure PMMA orientation. Three different orientation levels seem to be distinguishable. The two higher molecular weights

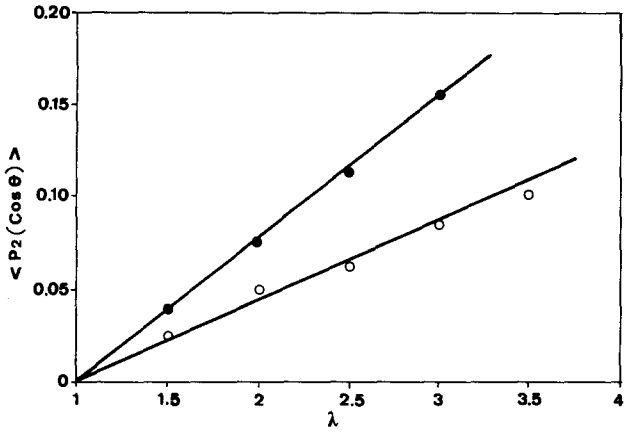

Figure 4 Orientation function of PMMA in PMMA (95%)–PEO (5%) blends as a function of draw ratio. Strain rate $\dot{\varepsilon}=0.115\,s^{-1}$. Temperature of stretching T:(●) 119°C; (○) 126°C

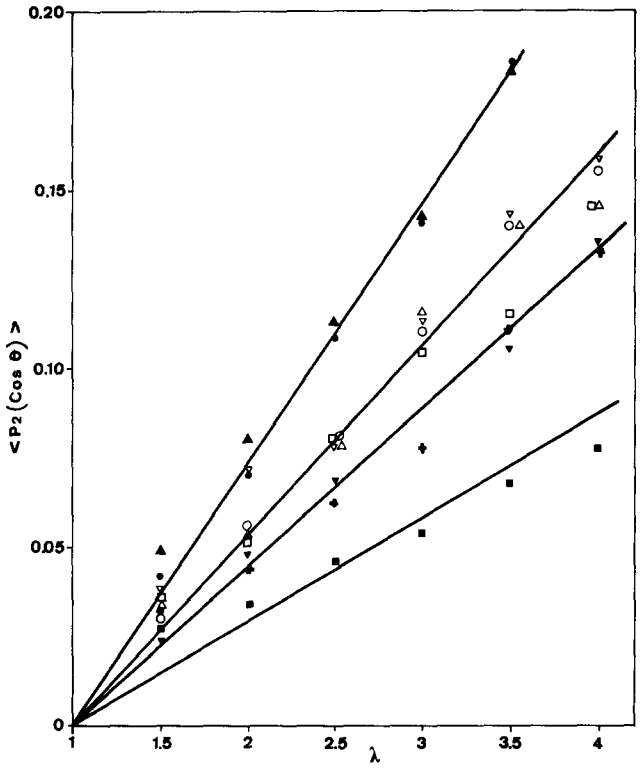

Figure 5 Orientation function of PMMA in PMMA (95%)–PEO (5%) blends as a function of draw ratio. PEO molecular weight: (+) 600; (▼) 1000; (□) 2000; (▽) 4000; (△) 20000; (○) 50000; (●) 200000; (▲) 600000; (■) pure PMMA. Temperature of stretching $T=T_g+23$°C. Strain rate $\dot{\varepsilon}=0.026\,s^{-1}$

(200000 and 600000) lead to the larger increase of PMMA orientation and cannot be differentiated from one another. A second level of orientation is reached when PEO molecular weight decreases. However, no influence of molecular weight on PMMA orientation is detectable in the range 2000–50000. A third level of PMMA orientation is obtained with PEO molecular weights 600 and 1000, PMMA orientation being, however, higher than pure PMMA orientation.

In *Figure 6* are given some results obtained in blends containing 10% of PEO. As previously observed, the general level of PMMA orientation is lowered and the influence of PEO molecular weight is similar to the behaviour observed in the 5% PEO blends.

All these results show that PEO molecular weight has a strong influence on PMMA orientation in the blends.

PEO orientation

As we have previously shown, the $\langle P_2(\cos\theta)\rangle$ orientation function of PEO cannot be obtained from infra-red measurements. On the other hand, although the intrinsic birefringence of PMMA is known ($\Delta^0_{PMMA} = -50.7\times10^{-4}$)[25], the intrinsic birefringence of amorphous PEO has not yet been measured. Thus it is impossible to measure the values of $\langle P_2(\cos\theta)\rangle_{PEO}$, but one can characterize PEO orientation by the function:

$$\langle P_2(\cos\theta)^*\rangle_{PEO} = \Delta^0_{PEO}\langle P_2(\cos\theta)\rangle_{PEO} = (\Delta - f\Delta^0_{PMMA}\langle P_2(\cos\theta)\rangle_{PMMA})/(1-f)$$

The values obtained experimentally for this function in the various blends studied, whatever the percentage and molecular weight of PEO, are very small ($\sim 3\times10^{-4}$) and independent of draw ratio.

Another way to estimate PEO orientation is to plot birefringence of the different blends studied as a function of PMMA orientation. The results, given in *Figure 7*, show that a rectilinear relation holds between Δ *versus* PMMA percentage $\times\ \langle P_2(\cos\theta)\rangle_{PMMA}$. The corresponding slope has a value -54.5×10^{-4}, which corresponds to PMMA intrinsic birefringence (-50.7×10^{-4}). As the intrinsic birefringence of amorphous PEO can be expected to be positive and much more important than Δ^0_{PMMA} (values of Δ^0_{PEO} between 3.5×10^{-2} and 3.75×10^{-2} in semicrystalline PEO oriented samples are reported in the literature[27]), the present results indicate

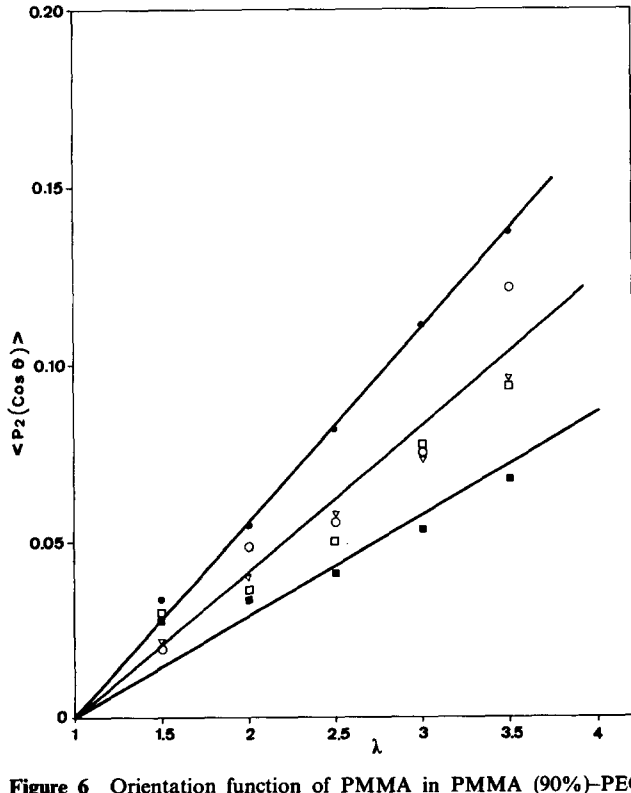

Figure 6 Orientation function of PMMA in PMMA (90%)–PEO (10%) blends as a function of draw ratio. PEO molecular weights: (□) 2000; (▽) 4000; (○) 50000; (●) 200000; (■); pure PMMA. Temperature of stretching $T=T_g+23$°C. Strain rate $\dot{\varepsilon}=0.026\,s^{-1}$

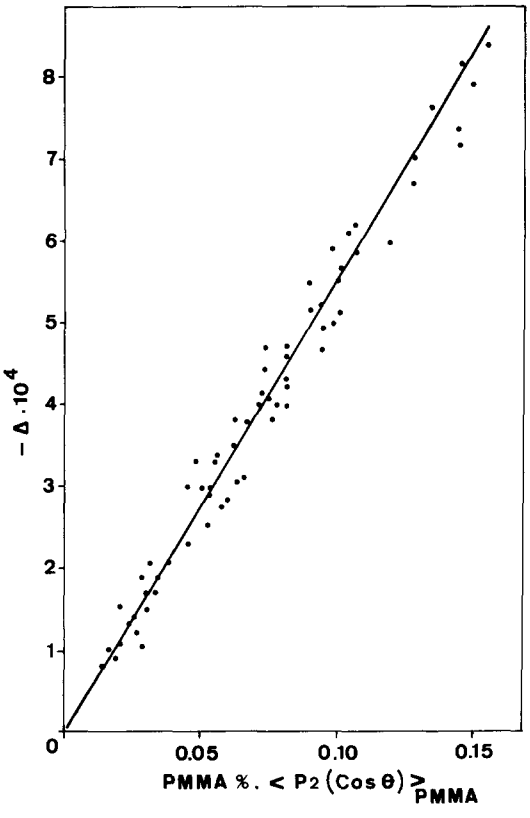

Figure 7 Birefringence of PMMA–PEO 20 blends as a function of PMMA percentage $\times \langle P_2(\cos\theta)\rangle_{PMMA}$

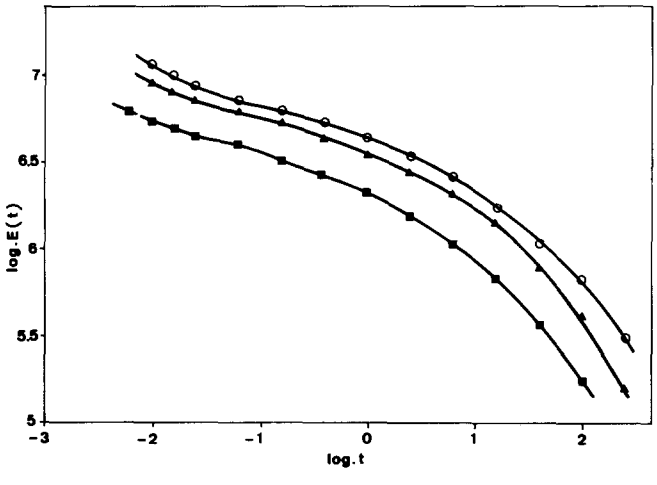

Figure 8 Master curves log $E(t)$ *versus* log t for PMMA–PEO 20 blends. Reference temperature $T=T_g+50°C$. PEO content: (■) 0%; (○) 5%; (▲) 10%

that no orientation of PEO chains occurs in the studied blends. Indeed, a slight orientation of PEO would induce in *Figure 8* a deviation from linearity on the higher absolute value side of birefringence, as we previously observed in PS–PVME blends at high draw ratios[4].

Viscoelasticity of PMMA–PEO blends

Mechanical relaxation curves can be deduced from dynamic shear experiments, which give the real $G'(\omega)$ and the imaginary $G''(\omega)$ parts of the complex modulus. The relaxation modulus can then be calculated from the formula of Ninomiya and Ferry[28]:

$$E(t)=G'(\omega)-0.4G''(0.4\omega)+0.014G''(10\omega)$$

with $\omega=1/t$.

For a given composition five different temperatures were swept. The time–temperature equivalence was used to reduce results to a reference temperature. Log $E(t)$ is plotted *versus* time t for pure PMMA and two PMMA–PEO 20 blends in *Figure 8* and for pure PMMA and three PMMA–PEO 4 blends in *Figure 9* at equivalent reference temperature $T=T_g+50°C$. The choice of this temperature is arbitrary but it falls within the range of experiments so no extrapolated reduction is necessary. The hindrance in relaxation in the blends is obvious. One can also notice that, in agreement with infra-red results, the mechanical relaxation is strongly hindered in the blends containing 5% of PEO. Then, when the PEO percentage increases, the hindrance in relaxation becomes less important.

From the experimental shift factor, log (a_{T/T_0}), one can calculate the WLF coefficients. The values obtained in the different blends studied are given in *Table 4* as well as the free volume fraction f_0 at the reference temperature $T_g+50°C$ and the thermal expansion coefficient of free volume α_f calculated from the relations[29]:

$$C_1^0=B/2.303f_0$$

$$C_2^0=f_0/\alpha_f$$

using a value of the constant $B=1$.

The values of the shift factor a_{T/T_0} obtained in the viscoelastic measurements can be used to obtain orientation relaxation master curves from the infra-red dichroism results. *Figure 10* relates to pure PMMA and blends containing 5% and 10% of PEO 20, stretched at a draw ratio $\lambda=2.5$ and at a reference temperature $T=T_g+10°C$.

One can notice again that PMMA is more oriented in

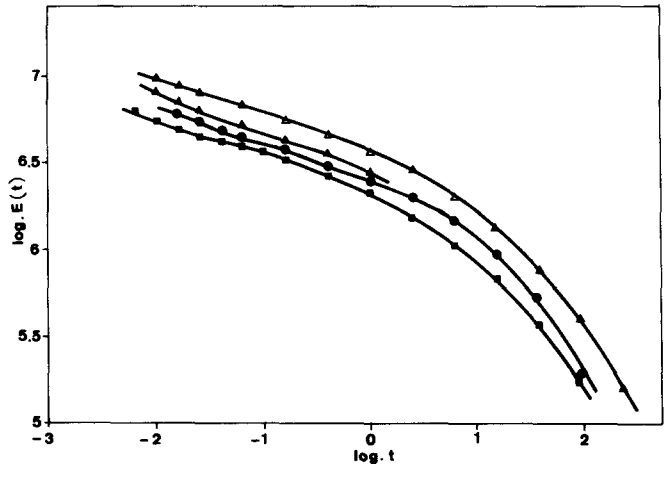

Figure 9 Master curves log $E(t)$ *versus* log t for PMMA–PEO 4 blends. Reference temperature $T=T_g+50°C$. PEO content: (■) 0%; (△) 5%; (▲) 10%; (●) 20%

Table 4 WLF parameters for different PMMA–PEO blends at the reference temperature $T=T_g+50°C$

Sample	C_1	C_2	f_0	α_f (K^{-1})
PMMA	8.54	131	0.051	3.9×10^{-4}
PMMA–PEO 20 (5%)	13.50	208.30	0.032	1.5×10^{-4}
PMMA–PEO 4 (5%)	10.40	156.70	0.042	1.5×10^{-4}
PMMA–PEO 20 (10%)	7.90	128.30	0.055	4.3×10^{-4}
PMMA–PEO 4 (10%)	7.90	137.40	0.055	4.0×10^{-4}
PMMA–PEO 4 (20%)	4.90	81.10	0.089	10.9×10^{-4}

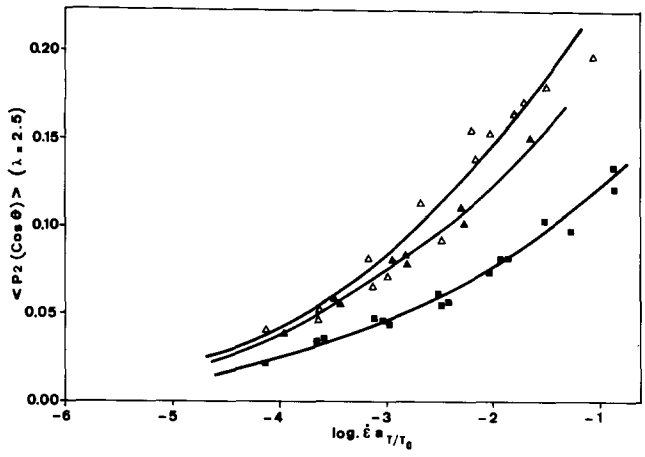

Figure 10 Master curve $\langle P_2(\cos\theta)\rangle_{PMMA}$ *versus* log $\dot{\varepsilon}a_{T/T_0}$ for PMMA–PEO 20 blends and a draw ratio $\lambda = 2.5$. PEO content: (■) 0%; (△) 5%; (▲) 10%. Reference temperature $T = T_g + 10°C$

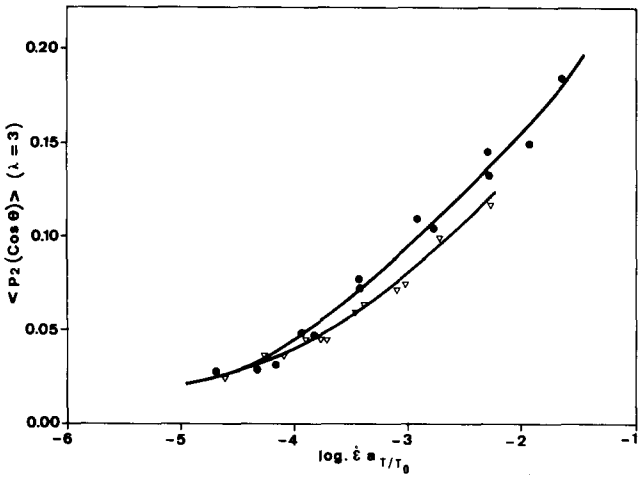

Figure 11 Master curve $\langle P_2(\cos\theta)\rangle_{PMMA}$ *versus* log $\dot{\varepsilon}a_{T/T_0}$ for PMMA (90%)–PEO (10%) blends and a draw ratio $\lambda = 3$. PEO molecular weight: (▽) 4000; (●) 20 000. Reference temperature $T = T_g + 10°C$

the blend than in the pure state. Furthermore, in the long relaxation time range, it is impossible to distinguish the two blends, while in the short relaxation time range, PMMA in the 5% blend is more oriented than in the 10% blend. One can also observe that the slope $d\langle P_2(\cos\theta)\rangle/d \log \dot{\varepsilon}a_{T/T_0}$ is larger in the blends than in pure PMMA in the short relaxation range.

Figure 11 relates to the influence of the PEO molecular weight on PMMA orientation relaxation. A slight influence of PEO molecular weight in the short relaxation time range is observed.

DISCUSSION

The present results show that, in PMMA–PEO blends containing up to 20% PEO, and stretched above the glass transition temperature, PMMA orientation is more important in the blend as compared to the pure polymer orientation stretched under the same conditions (same $T - T_g$ and $\dot{\varepsilon}$). This increase of PMMA orientation in the blends cannot be related to an increase of chain entanglement. Indeed Wu[30] has recently shown that in different compatible blends, including PMMA–PEO blends, the specific interactions tend to align the chain segments for the interactions, thus locally stiffening the segments, reducing their convolution and resulting in reduced entanglements between dissimilar chains. Such a stiffening was experimentally observed by *FT* i.r. spectroscopy[31] on thin films. The results show that, in PMMA–PEO blends, PEO chains preferentially take a planar zig-zag structure.

As a matter of fact, similarly to the previous compatible blends studied, the increase of PMMA orientation in PMMA–PEO blends can be interpreted in terms of hindrance of relaxation of PMMA chains induced by a modification of friction coefficients due to the molecular interactions. As far as PEO is concerned, this polymer has a very short relaxation time, which is not in the time range covered in the experimental conditions, and no orientation can be observed. A similar behaviour was found for PVME in PS–PVME blends[4]. However, the comparison of PMMA–PEO blends with the other blends previously studied shows that, in the present case, PMMA–PEO blends behave differently. Instead of a regular increase of PMMA orientation with increasing amount of PEO, followed eventually by a plateau, PMMA orientation goes through a maximum for a concentration of 5% PEO, then regularly decreases to reach the value of pure PMMA orientation in the blend containing 20% PEO. It seems that this peculiar behaviour could be assigned to the beginning of phase separation. Indeed, different studies suggest that such a process takes place. Recently, in our laboratory, an n.m.r. study on compatibility of PMMA–PEO blends[32] has pointed out that blends containing at least 10% PEO are not homogeneous at room temperature. Besides an amorphous phase of PMMA–PEO, one can observe an amorphous phase of almost pure PEO. Such microphase separation is not observed in 5% PEO blends. Using thermal analysis one can observe structural changes in the 20% PEO blend after ageing for ten months at room temperature. As shown in *Figure 12* a thermal treatment of two days at 40°C almost generates the initial structure. Thermal analysis of the same blend stretched at 87°C, strain rate $\dot{\varepsilon} = 0.026\ s^{-1}$ and draw ratio $\lambda = 2.5$ (*Figure 13*) clearly shows an endothermic peak around 60°C. After heating up to 160°C this peak disappears and the initial structure is regenerated. At least, small-angle neutron scattering experiments performed on oriented

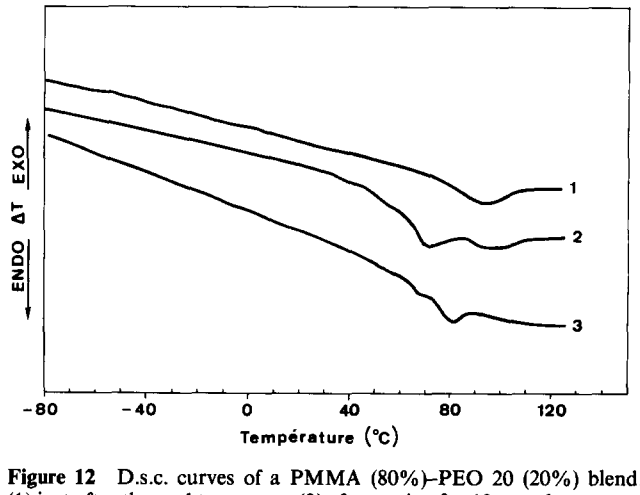

Figure 12 D.s.c. curves of a PMMA (80%)–PEO 20 (20%) blend; (1) just after thermal treatment; (2) after ageing for 10 months at room temperature; (3) sample 2 heated for two days at 40°C

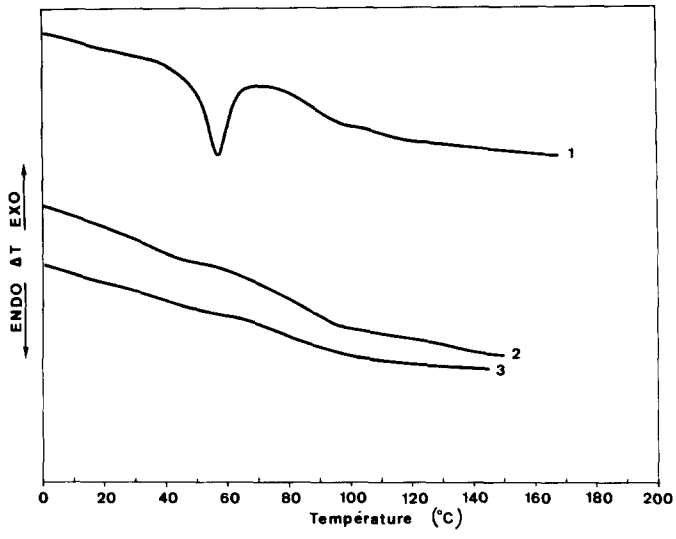

Figure 13 D.s.c. curves of a PMMA (80%)–PEO 20 (20%) blend stretched at $T=87°C$, strain rate $\dot{\varepsilon}=0.026\,s^{-1}$ and draw ratio $\lambda=2.5$: (1) first run; (2) second run; (3) third run

samples containing 10% PEO[19] demonstrate that phase separation occurs.

When the blends containing at least 10% PEO are heated above T_g before stretching, both polymers are compatible and the true T_g of the blend is lower than the T_g measured from room temperature on samples that present microphase separation. As stretching experiments were carried out at constant $T-T_g$ differences, where T_g is the temperature measured from room temperature, the samples are in fact stretched at a higher temperature than expected. The strong dependence of orientation on the stretching temperature results in an important lowering of the orientation compared to the blends containing 5% PEO, which do not present any microphase separation. For these 5% PEO blends, the T_g measured from room temperature is the true T_g. The master curves of the real (G') and imaginary (G'') parts of the complex modulus in the blends containing 5% and 10% PEO, at a reference temperature $T=T_g+50°C$, are given in *Figure 14*. A change of 6°C in the value of T_g of the 10% PEO blend, i.e. a reference temperature $T=T_g+44°C$, is enough to make the two curves coincide.

As far as the influence of PEO molecular weight is concerned, an increase of molecular weight induces an increase of PMMA orientation, although PEO chains remain unoriented. This effect could be tentatively explained by a cooperative effect of interactions between PMMA and PEO chains increasing with PEO molecular weight. However, in the case of the highest molecular weights the influence of entanglements between PEO chains cannot be excluded. In a blend, the critical mass M_c for PEO chain self-entanglements is given by the relation[33]:

$$M_c = M_c^0/f$$

where f is the PEO concentration in the blend and M_c^0 the critical mass of pure PEO. According to Aharoni[34] $M_c^0=4400$. In the 5% and 10% PEO blends M_c has the values 88 000 and 44 000. The experimental results show that entanglements may play a role in the PEO 200 and PEO 600 blends. In blends based on lower-molecular-weight PEO ($2000 \leqslant M_w \leqslant 50\,000$), no influence can be pointed out in the limit of experimental errors. In the

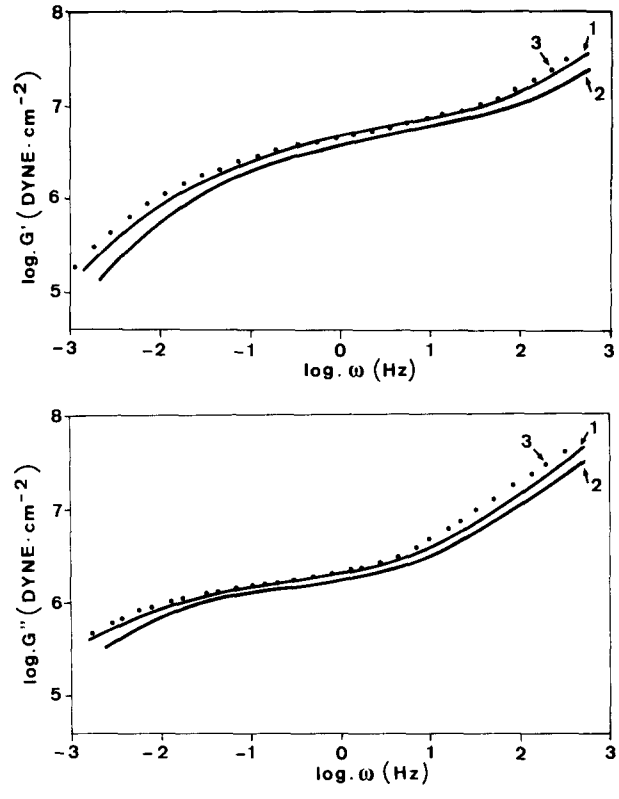

Figure 14 Master curves log G' and log G'' *versus* log ω for PMMA–PEO 20 blends: (1) PMMA (95%)–PEO (5%) blend at reference temperature $T=T_g+50°$; (2) PMMA (90%)–PEO (10%) blend at reference temperature $T=T_g+50°C$; (3) PMMA (90%)–PEO (10%) blend at reference temperature $T=T_g+44°C$

case of the two PEO of lower molecular weight (PEO 06 and PEO 1), one observes a different behaviour. These blends present a lowering of the glass transition temperature (see *Table 3*) and PMMA orientation is influenced neither by PEO percentage (up to 10%) nor by PEO molecular weight (up to 1000). In this range of molecular weights, PEO chains can act as a plasticizer unable to lead to a cooperative effect of interchain interaction points. As a matter of fact, the influence of these low-molecular-weight PEO on PMMA orientation is identical to the influence observed when tetraethyleneglycol dimethyl ether is used as a plasticizer[35].

REFERENCES

1 Lefebvre, D., Jasse, B. and Monnerie, L. *Polymer* 1982, **23**, 706
2 Lefebvre, D., Jasse, B. and Monnerie, L. *Polymer* 1983, **24**, 1240
3 Lefebvre, D., Jasse, B. and Monnerie, L. *Polymer* 1984, **25**, 318
4 Faivre, J. P., Jasse, B. and Monnerie, L. *Polymer* 1985, **26**, 879
5 Faivre, J. P., Xu, Z., Halary, J. L., Jasse, B. and Monnerie, L. *Polymer* 1987, **28**, 1881
6 Bouton, C., Arrondel, V., Rey, V., Jasse, B. and Monnerie, L. *Polymer* 1989, **30**, 1414
7 Sanchez, I. C. 'Polymer Blends', Academic Press, New York, 1978
8 Martuscelli, E. and Demma, G. 'Polymer Blends: Processing, Morphology and Properties', Plenum Press, New York, 1980
9 Martuscelli, E., Canetti, M., Vicini, L. and Seves, A. *Polymer* 1982, **23**, 33
10 Martuscelli, E., Pracella, M. and Wang, P. Y. *Polymer* 1984, **25**, 1097
11 Martuscelli, E., Silvestre, C., Addonizio, M. L. and Amelino, L. *Makromol. Chem.* 1986, **187**, 1557
12 Martuscelli, E., Demma, G., Rossi, E. and Serge, A. L. *Polym. Commun.* 1983, **24**, 266
13 Nishi, T. and Wang, T. T. *Macromolecules* 1975, **8**, 909

14 Cortazar, M. M., Calahorra, M. E. and Guzman, G. M. *Eur. Polym. J.* 1982, **18**, 165
15 Liberman, S. A. and Gomes, A. S. *J. Polym. Sci., Polym. Phys. Edn.* 1984, **22**, 280
16 Alfonso, G. C. and Russell, T. P. *Macromolecules* 1986, **19**, 1143
17 Hoffman, D. M. Ph.D. Thesis, University of Massachusetts, 1979
18 Li, X. and Hsu, S. L. *J. Polym. Sci., Polym. Phys. Edn.* 1984, **22**, 1331
19 Lefebvre, J. M. R., Porter, R. S. and Wignall, G. D. *Polym. Eng. Sci.* 1987, **27**, 433
20 Fajolle, R., Tassin, J. F., Sergot, Ph., Pambrun, Cl. and Monnerie, L. *Polymer* 1983, **24**, 379
21 Shindo, Y. and Hanabusa, H. *Polym. Commun.* 1983, **24**, 240
22 Badoz, J., Billardon, M., Canit, J. C. and Russel, M. F. *J. Opt. (Paris)* 1977, **8**, 373
23 Ward, I. M. 'Structure and Properties of Oriented Polymers', Applied Science, London, 1975
24 Nagai, H. *J. Appl. Polym. Sci.* 1963, **7**, 1697
25 Zhao, Y., Jasse, B. and Monnerie, L. *Makromol. Chem., Macromol. Symp.* 1986, **5**, 87
26 Weiner, O. *Abk. Kgl. Sachs. Ges. Wiss. Math. Phys. Kl* 1972, **32**, 509
27 Kim, B. S. and Porter, R. S. *Macromolecules* 1985, **18**, 1214
28 Ninomiya, K. and Ferry, J. D. *J. Colloid Sci.* 1959, **14**, 36
29 Ferry, J. D. 'Viscoelastic Properties of Polymers', 3rd Edn., Wiley, New York, 1980
30 Wu, S. *J. Polym. Sci., Polym. Phys. Edn.* 1987, **25**, 2511
31 Rao, G. R., Castiglioni, C., Gussoni, M., Zerbi, G. and Martuscelli, E. *Polymer* 1985, **26**, 811
32 Panizel, N. Thesis, Paris, 1988
33 Kotaka, T. and Watanabe, H. *Makromol. Chem. Suppl.* 1985, **14**, 179
34 Aharoni, S. M. *Macromolecules* 1986, **19**, 426
35 Zhao, Y. Thesis, Paris, 1987